The Astrophysical Journal, 668:L115–L118, 2007 October 20

THE EVOLVING FAINT END OF THE LUMINOSITY FUNCTION

S. Khochfar,[1] J. Silk,[1] R. A. Windhorst,[2] and R. E. Ryan, Jr.[3]

Received 2007 July 16; accepted 2007 August 27; published 2007 October 2

ABSTRACT

We investigate the evolution of the faint-end slope of the luminosity function, α, using semianalytical modeling of galaxy formation. In agreement with observations, we find that the slope can be fitted well by $\alpha(z) = a + bz$, with $a = -1.13$ and $b = -0.1$. The main driver for the evolution in α is the evolution in the underlying dark matter mass function. Sub-L_* galaxies reside in dark matter halos that occupy a different part of the mass function. This part of the mass function is steeper at high redshifts than at low redshifts, and hence α is steeper. Supernova feedback in general causes the same relative flattening with respect to the dark matter mass function. The faint-end slope at low redshifts is dominated by field galaxies, and at high redshifts by cluster galaxies. The evolution of $\alpha(z)$ in each of these environments is different, with field galaxies having a slope $b = -0.14$ and cluster galaxies having a slope $b = -0.05$. The transition from a cluster-dominated to a field-dominated faint-end slope occurs roughly at a redshift $z_* \simeq 2$ and suggests that a single linear fit to the overall evolution of $\alpha(z)$ might not be appropriate. Furthermore, this result indicates that tidal disruption of dwarf galaxies in clusters cannot play a significant role in explaining the evolution of $\alpha(z)$ at $z < z_*$. In addition, we find that different star formation efficiencies a_* in the Schmidt-Kennicutt law and supernova-feedback efficiencies ϵ generally do not strongly influence the evolution of $\alpha(z)$.

Subject headings: galaxies: evolution — methods: numerical

1. INTRODUCTION

The galaxy luminosity function (LF) is one of the cornerstones in our understanding of galaxy formation and evolution. Since the introduction of a fitting function for its shape by Schechter (1976), the origin of the form of the LF function has been a powerful constraint on model building (e.g., Benson et al. 2003; Samui et al. 2007). While recent work has focused somewhat on the luminous end, its evolution with redshift (Brown et al. 2007), and the role of dry mergers (Khochfar & Burkert 2003; Naab et al. 2006), the faint end provides additional important clues on galaxy formation. Systematic studies of the faint-end slope in the local universe reveal differences between high- and low-density environments (Trentham 1998), as well as between galaxy samples split by morphologies (e.g., Marzke et al. 1994). The underlying physical processes that shape the faint end of the luminosity function are generally associated with feedback from supernovae that is effective in heating gas and driving winds in shallow gravitational potentials (Dekel & Silk 1986). Although the implementation of supernova feedback in galaxy formation models has been extensively investigated (e.g., Benson et al. 2003) for the local galaxy luminosity function, its impact on the redshift evolution on the faint end has not been as well studied. The recent wealth of luminosity functions measured to very faint magnitudes in the rest-frame B band (e.g., Blanton et al. 2003; Wolf et al. 2003; Marchesini et al. 2007; Ryan et al. 2007) and in the rest-frame far-ultraviolet (FUV; e.g., Yan & Windhorst 2004b; Wyder et al. 2005; Bouwens et al. 2006) allows us to test models with high accuracy.

The purpose of this Letter is to investigate the underlying driving mechanism for the redshift evolution of the faint-end slope. Furthermore, we investigate the impact of supernova feedback on the rate of star formation by varying the relevant efficiency parameters.

2. MODEL

In the following we briefly outline our basic modeling approach and refer the reader for more details to Khochfar & Burkert (2005), Khochfar & Silk (2006), and reference therein. We generate merger trees for dark matter halos using a Monte Carlo approach based on the extended Press-Schechter formalism (Somerville & Kolatt 1999). As we aim to model the faint end of the LF to high redshifts, we need to make sure that the mass resolution in our simulations is sufficient. We generate merger trees from dark matter mass functions between $z = 0$ and $z = 6$, and we find that resolving each individual merger tree down to a mass resolution of $M_{\rm min} = 5 \times 10^9\, M_\odot$ and $M_{\rm min} = 10^8\ M_\odot$ at $z \leq 3$ and $z \geq 4$, respectively, gives robust results. Once a tree reaches $M_{\rm min}$, we start moving the tree forward in time, including physical processes associated with the baryons within each dark matter halo that include gas cooling, star formation, supernova feedback, reionization, and merging of galaxies on a dynamical friction timescale. As the focus of this Letter is on the faint end of the luminosity function, we will omit including prescriptions for active galactic nucleus feedback (e.g., Bower et al. 2006) or environmental effects (Khochfar & Ostriker 2007) that mainly influence the bright end of the luminosity function.

The largest impact on the slope at the faint end comes from star formation and associated supernova feedback (Dekel & Silk 1986). Faint galaxies generally occupy small dark matter halos with shallow potential wells, which allow effective reheating of cold gas in the interstellar medium (ISM) by feedback from supernovae. We model star formation in galaxies using a parameterization of the global Schmidt-Kennicutt law (Kennicutt 1998) according to which $\dot{M}_* = a_* M_{\rm cold}/t_{\rm dyn}$, where a_* is a free parameter that is indicative of the efficiency of star formation, $M_{\rm cold}$ is the mass in cold gas in the galactic disk, and $t_{\rm dyn}$ is the dynamical timescale of the galaxy. Following

[1] Department of Physics, Denys Wilkinson Building, University of Oxford, Keble Road, Oxford OX1 3RH, UK; sadeghk@astro.ox.ac.uk, silk@astro.ox.ac.uk.

[2] School of Earth and Space Exploration, Arizona State University, Tempe, AZ 85287; Rogier.Windhorst@asu.edu.

[3] Department of Physics, Arizona State University, Tempe, AZ 85287; Russell.Ryanjr@asu.edu.

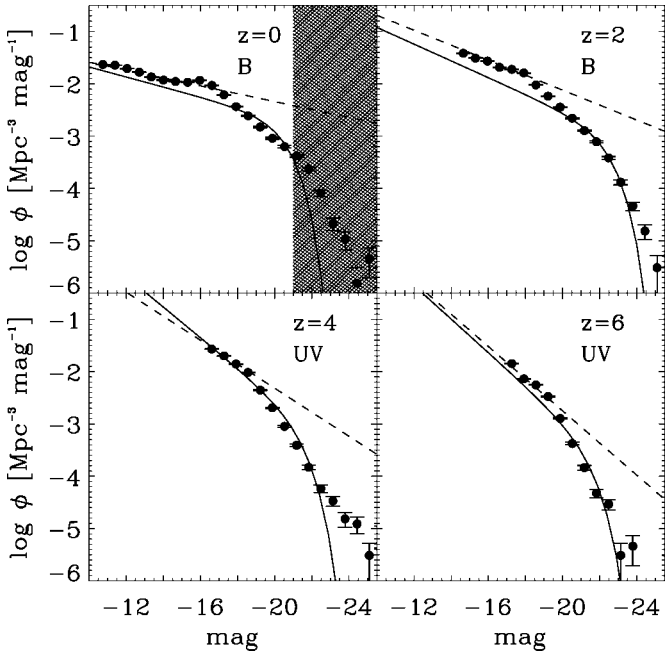

FIG. 1.—Comparison between model luminosity functions with $\epsilon = 0.6$ and $\alpha = 0.02$ (*filled circles*) and Schechter fits to various observations of the luminosity function at different redshifts (*solid lines*). The dashed lines show our power-law fits to the faint end of the LF. *Top left panel*: Rest-frame *B*-band luminosity function from Norberg et al. (2002), where we assumed that $B = b_j + 0.12$ mag. The shaded area indicates the region of the luminosity function that is not well matched due to missing feedback effects. *Top right panel*: Rest-frame *B*-band luminosity function from Marchesini et al. (2007). *Bottom left panel*: UV luminosity function from Bouwens et al. (2007). *Bottom right panel*: UV luminosity function from Yan & Windhorst (2004a). Following Bouwens et al. (2006), we assume an average dust correction of 0.4 mag at $z \geq 4$.

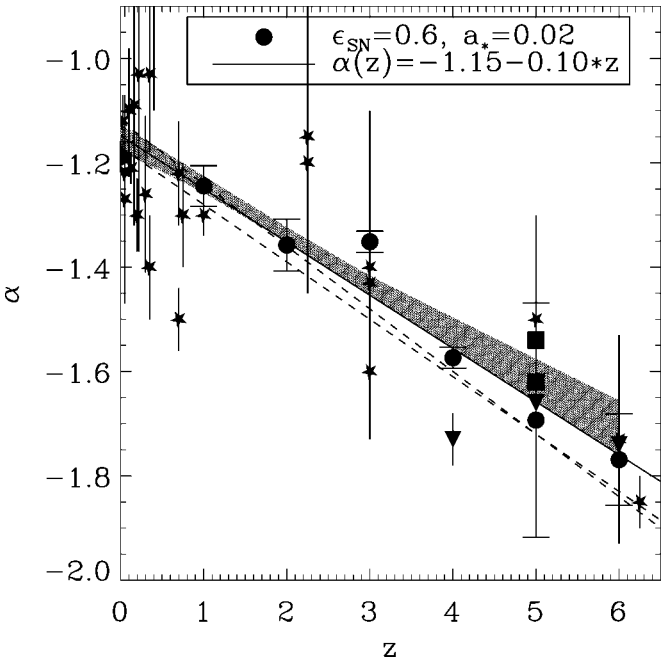

FIG. 2.—Slope α at different redshifts, as predicted by the best-fit local model with $a_* = 0.02$ and $\epsilon = 0.6$. The filled symbols show the results from the simulation, and the solid line is the best fit to the simulation data. Error bars indicate 1 σ errors. The dashed lines show the fit to the compiled data in Ryan et al. (2007). The shaded region shows the range of linear fits to $\alpha(z)$ that we find when varying the star formation and supernova feedback efficiencies, as discussed in the text. The filled stars are the compilation from Ryan et al. (2007). The filled squares and triangles show recent results from Oesch et al. (2007) and Bouwens et al. (2007), respectively.

the arguments of Dekel & Silk (1986), we model the amount of cold gas reheated by feedback from supernovae with $M_{\rm SN} = 4\epsilon M_* \eta_{\rm SN} E_{\rm SN}/3V_{\rm max}^2$, where ϵ is a free parameter that controls the feedback efficiency, $\eta_{\rm SN}$ is the number of supernovae per solar mass of stars formed, $E_{\rm SN} = 10^{51}$ ergs is the energy released by each supernova, and $V_{\rm max}$ is the maximum circular velocity of the dark matter halo in which the galaxy resides.

For each individual galaxy in our simulation, we store the star formation history and generate its *B*-band and FUV rest-frame luminosity function at various redshifts using the stellar population models of Bruzual & Charlot (2003). The faint end of the luminosity function is then fitted by a simple power law with slope α as defined in Schechter (1976). We fit the faint-end LF at each redshift with a power law spanning a range of 4 mag at $z \leq 3$ and at least 2 mag at $z > 3$, starting at the lowest magnitude $L_{\rm min}$ that is unaffected by the mass resolution of the simulation. We choose this approach over fitting the whole LF with a Schechter fit because we are missing physical effects (see below) in our model that are responsible for shaping the bright end and the knee of the LF. In addition, we increase the number of magnitude bins and make sure that the fitted values for α are unaffected by the bin size. Figure 1 shows the luminosity function at magnitudes larger than the corresponding minimum magnitude for $L_{\rm min}$. In this study, we simulate a volume of 10^6 Mpc^3, which allows us to calculate α robustly up to a redshift $z \simeq 6$.

Throughout this Letter, we use the following set of cosmological parameters based on the three-year *Wilkinson Microwave Anisotropy Probe* data (Spergel et al. 2007): $\Omega_0 = 0.27$, $\Omega_\Lambda = 0.73$, $\Omega_b/\Omega_0 = 0.17$, $\sigma_8 = 0.77$, and $h = 0.71$.

3. RESULTS

There is significant evidence that the faint-end slope of the galaxy luminosity function shows a measurable dependence on redshift, which can be fitted by a linear law of the form $\alpha(z) = a + bz$, with a between -1.12 and -1.17, and b between -0.12 and -0.11 (for recent observations, see Sawicki & Thompson 2006, Marchesini et al. 2007, and Ryan et al. 2007). Within the hierarchical structure formation paradigm, one naturally expects such behavior, considering that the slope of the dark matter mass function below $M_{\rm DM,*}$ is $\alpha_{\rm DM} \sim 2$ and that the objects that form in these halos continue to grow by continued star formation and mergers with each other (Khochfar & Burkert 2001), hence flattening the slope. Figure 1 shows the predicted model luminosity function at various redshifts in the rest-frame *B* and UV. The simulated and observed luminosity functions are in fair agreement at the faint end. The luminous end, however, shows deviations at low redshift that are due to missing feedback sources in massive galaxies such as active galactic nuclei or to environmental effects. In Figure 2, we show the predicted evolution of $\alpha(z)$ for our best-fit local model. The free parameters a_* and ϵ in this model are chosen to give the best fit to various local observations (see Khochfar & Silk 2006). For consistency with the majority of observations, we calculate the faint-end slope for the rest-frame FUV at $z \geq 4$ and for the rest-frame *B* band at lower redshifts. We indeed find an evolution in α with redshift that is in fair agreement with the observed evolution.

What is the main driver for the evolution in α, and what

influences it? Generally, supernova feedback is considered the dominant mechanism in shaping the faint end of the luminosity function (Dekel & Silk 1986; Benson et al. 2003). The shaded region in Figure 2 shows the range of linear fits to $\alpha(z)$ that we find by varying the star formation efficiency between $a_* = 0.02$ and 0.1 and the supernova feedback efficiency between $\epsilon = 0.2$ and 0.6. We infer only a very modest change in $\alpha(z)$ for reasonable choices of feedback efficiencies, and therefore we conclude that another process must be responsible for the observed evolution in $\alpha(z)$.

The mass function of dark matter halos is known to show a strong evolution with redshift (e.g., Press & Schechter 1974). The galaxies contributing to the luminosity function around L_* are mostly central galaxies in their dark matter halos, i.e., the most luminous galaxy within the halo (e.g., Khochfar & Ostriker 2007). It is therefore not unreasonable to assume a connection between the evolution of $\alpha(z)$ and that of the dark matter mass function. When considering the luminosity of central galaxies residing in dark matter halos of the same mass at different redshifts, we find that at early times, central galaxies are up to 3 mag brighter than their counterparts in low-redshift halos. This is even the case for halos hosting sub-L_* galaxies. Similar results have been reported by Kobayashi et al. (2007), who showed that dwarf galaxies at early times are not affected by supernova feedback in their simulations because cooling times are very short in these halos and because the energy injected by the supernovae is rapidly dissipated away. The slope in the region of dark matter halos that host sub-L_* galaxies is steeper at high redshift, and consequently so is α. The same is true for other choices of a_* and ϵ, thereby explaining why we do not find any strong dependence of $\alpha(z)$ on these parameters. It should be noted, however, that modeling these parameters with a strong redshift dependency will enhance or weaken the evolution of α.

We continue analyzing the evolution in $\alpha(z)$ by distinguishing between cluster and field galaxies and their relaxation to the overall luminosity function at the faint end. In Figure 3, we present $\alpha(z)$ for progenitor galaxies of present-day cluster and field galaxies from our simulations. Here we define cluster environments as present-day dark matter halos above $10^{14}\,M_\odot$ and field environments as halos with masses below $10^{12}\,M_\odot$; α is steeper and evolves more strongly in field environments than in cluster environments. At early times, the first galaxies to appear are most likely in high-σ fluctuations, which will result in present-day galaxy clusters. Consequently, the faint-end luminosity function at high redshifts will be dominated by present-day cluster members, and the faint-end slope of the overall galaxy population at high redshifts is flatter than that for the field luminosity function alone at the same redshift. When considering the relative weight of field galaxies to the overall galaxy population at the faint end, one can estimate the redshift at which the transition from cluster-driven to field-driven evolution in α occurs. We find that this transition roughly occurs at $z_* \simeq 2$, with a slight dependency on the definition of environment.

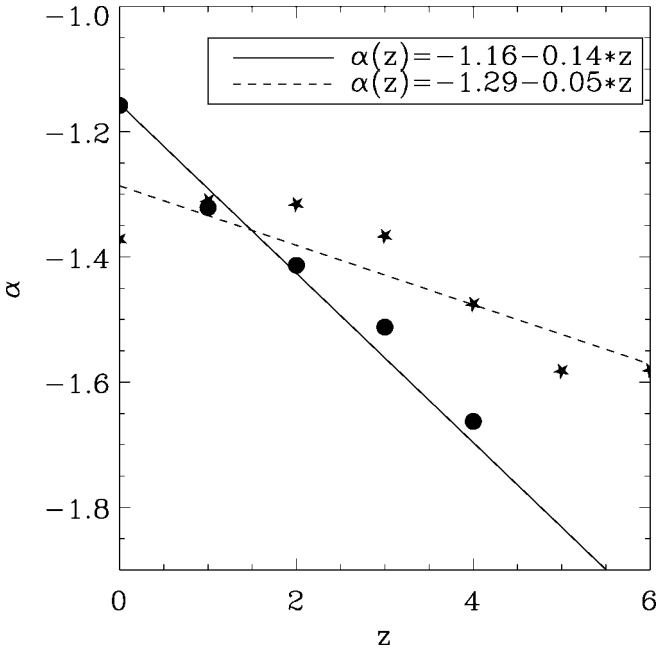

FIG. 3.—Slope α at different redshifts, as predicted by the best-fit local model. The filled circles show the results for typcal field environments, and the filled stars show the results for cluster environments, as defined by their present-day dark halo mass. The solid and dashed lines are the fits to the modeled evolution in the field and cluster, respectively. Here we define cluster environments as present-day dark matter halos above $10^{14}\,M_\odot$ and field environments as halos with masses below $10^{12}\,M_\odot$.

4. DISCUSSION AND CONCLUSIONS

In this Letter, we presented predictions for the redshift evolution of the faint-end slope of the luminosity function within the ΛCDM scenario. In general, we find the same trend as in the recent observations, i.e., a steepening faint-end slope α with redshift, which can be well fitted by a simple linear fit $\alpha(z) = a + bz$, where the observations find that $a \simeq 1.17$ and $b \simeq -0.11$ (Ryan et al. 2007). Our simulations predict $a \simeq 1.13$ and $b \simeq -0.1$, in good agreement with the observations, considering the large uncertainties, especially at high redshifts.

Our simulations confirm previous results that the flattening of the faint-end slope α with respect to the slope in the dark matter mass function can be well explained by supernova feedback. In addition, however, we show that α is steeper at higher redshifts mainly, due to the dark matter mass function being steeper for the range of halo masses that host sub-L_* galaxies, suggesting that the evolution of α traces closely that of the underlying dark matter mass function.

The contribution of the progenitor population of present-day field and cluster galaxies plays a significant role in shaping the evolution of α. The evolution of $\alpha(z)$ is stronger for field galaxies, with $b = -0.14$ and $a = -1.16$, than for cluster galaxies. In our simulations, we find that at redshifts $z \geq 2$, the faint end is dominated by galaxies that end up in present-day clusters. This transition redshift is dependent on the value of σ_8, which normalizes the power spectrum and regulates the redshift at which structures of a given mass typically form. In addition, the slope of the fluctuation spectrum at small scales will influence z_*. Precise high-redshift measurements of the contributions of these two populations to the faint end of the luminosity function in future surveys with, e.g., the *Hubble Space Telescope* (*HST*) Wide Field Camera 3, will help us to pin down z_*. One potential problem for future surveys will be the possible bias toward cluster galaxies, as they might experience induced star formation (Marcillac et al. 2007), increasing their surface brightness and making them more easily detectable. This effect will shift z_* to higher redshifts and needs to be carefully taken into account. Observational selection effects will affect the observed faint-end LF slope shown in Figure 2. Some observational selection effects (e.g., catalog incompleteness and natural confusion; Windhorst

et al. 2007) can make the observed faint-end slope flatter than the true one, while others (e.g., surface brightness dimming) could make the observed slope somewhat steeper than the true one, depending on the exact intrinsic object size distribution. A number of groups correct for incompleteness either through Monte Carlo simulations (e.g., Yan & Windhorst 2004a) or through cloning techniques (e.g., Bouwens et al. 2006) and find similar faint-end slopes when following different procedures. When judging the data, however, one must keep these observational biases in mind. Ultimately, these issues can only be resolved with deeper *James Webb Space Telescope* (*JWST*) data to AB = 31–32 mag.

Tidal disruption of dwarf galaxies in clusters as seen in high-resolution simulations (Tormen et al. 1998) can in principle change the slope α. Our results, however, suggest that at a transition redshift of $z_* = 2$, the evolution of α changes from being dominated by cluster galaxies to being dominated by field galaxies. It is therefore not likely that a large amount of the evolution in α at $z < z_*$ is driven by tidal disruption of faint galaxies. An additional implication from the transition at z_* is that the evolution of $\alpha(z)$ is better fit by a linear function with a break at z_*.

The flattening of the slope α with respect to the underlying dark matter slope suggests the interesting possibility of estimating the timescale over which supernovae operate. Assuming that the first Population II stars were formed sometime before reionization (Yan & Windhorst 2004a), and that supernovae Type Ia originate roughly $\leq$1–2 Gyr after the bulk of the first Population II star formation, one would expect an increase in energy injection into the ISM at a redshift corresponding to this time lag. This additional energy input will hinder star formation and contribute to a further increase in the mass-to-light ratio of galaxies, and hence to an even stronger flattening of the slope α. It will be crucial to have robust measurements of α over a wide range of redshifts, to probe the onset of the first significant feedback contribution from Type Ia supernovae. Furthermore, probing the faint-end slope at redshifts $z > 6$, before the significant onset of Type II supernovae, will allow us to measure the underlying dark matter slope very accurately.

Our approach has certain shortcomings. The model presented here did not include any time delay prescriptions for the various types of supernovae (SNe) but instead assumed instantaneous feedback. More detailed modeling of the time delays and their influence on the faint-end slope will be presented elsewhere (S. Khochfar et al., in preparation). Our treatment of SN feedback is very simplistic, and more detailed hydrodynamical simulations, including a multiphase medium, will show whether or not this general trend that we report can be recovered. Indeed, first generations of such simulations show that Type II SNe that are generated in dense star clusters explode into bubbles of hot gas and are therefore less efficient at feedback into the ISM (Mac Low & Ferrara 1999) than Type Ia SNe, which go off at random places in the galaxy and can have more of an effect on the early ISM.

We would like to thank Seth Cohen, Evan Scannapieco, and Richard Bouwens for helpful discussions and the anonymous referee for his useful comments. This work was supported by *HST* grants HST-GO-10530.07 (to R. A. W.) and HST-AR-10974.01 (to R. E. R.) from STScI, which is operated by AURA, Inc., for NASA under contract NAS 5-26555, and by NASA *JWST* grant NAG 5-12460 (to R. A. W.).

REFERENCES

Benson, A. J., Bower, R. G., Frenk, C. S., Lacey, C. G., Baugh, C. M., & Cole, S. 2003, ApJ, 599, 38
Blanton, M. R., et al. 2003, ApJ, 592, 819
Bouwens, R. J., Illingworth, G. D., Blakeslee, J. P., & Franx, M. 2006, ApJ, 653, 53
Bouwens, R. J., Illingworth, G. D., Franx, M., & Ford, H. 2007, ApJ, in press (astro-ph/0707.2080)
Bower, R. G., Benson, A. J., Malbon, R., Helly, J. C., Frenk, C. S., Baugh, C. M., Cole, S., & Lacey, C. G. 2006, MNRAS, 370, 645
Brown, M. J. I., Dey, A., Jannuzi, B. T., Brand, K., Benson, A. J., Brodwin, M., Croton, D. J., & Eisenhardt, P. R. 2007, ApJ, 654, 858
Bruzual, G., & Charlot, S. 2003, MNRAS, 344, 1000
Dekel, A., & Silk, J. 1986, ApJ, 303, 39
Kennicutt, R. C., Jr. 1998, ApJ, 498, 541
Khochfar, S., & Burkert, A. 2001, ApJ, 561, 517
———. 2003, ApJ, 597, L117
———. 2005, MNRAS, 359, 1379
Khochfar, S., & Ostriker, J. P. 2007, ApJ, submitted (astro-ph/0704.2418)
Khochfar, S., & Silk, J. 2006, MNRAS, 370, 902
Kobayashi, C., Springel, V., & White, S. D. M. 2007, MNRAS, 376, 1465
Mac Low, M.-M., & Ferrara, A. 1999, ApJ, 513, 142
Marchesini, D., et al. 2007, ApJ, 656, 42
Marcillac, D., Rigby, J. R., Rieke, G. H., & Kelly, D. M. 2007, ApJ, 654, 825
Marzke, R. O., Geller, M. J., Huchra, J. P., & Corwin, H. G., Jr. 1994, AJ, 108, 437
Naab, T., Khochfar, S., & Burkert, A. 2006, ApJ, 636, L81
Norberg, P., et al. 2002, MNRAS, 336, 907
Oesch, P. A., et al. 2007, ApJ, submitted (astro-ph/0706.2653)
Press, W. H., & Schechter, P. 1974, ApJ, 187, 425
Ryan, R. E., Jr., et al. 2007, ApJ, in press (astro-ph/0703743)
Samui, S., Srianand, R., & Subramanian, K. 2007, MNRAS, 377, 285
Sawicki, M., & Thompson, D. 2006, ApJ, 648, 299
Schechter, P. 1976, ApJ, 203, 297
Somerville, R. S., & Kolatt, T. S. 1999, MNRAS, 305, 1
Spergel, D. N., et al. 2007, ApJS, 170, 377
Tormen, G., Diaferio, A., & Syer, D. 1998, MNRAS, 299, 728
Trentham, N. 1998, MNRAS, 294, 193
Windhorst, R. A., Hathi, N. P., Cohen, S. H., Jansen, R. A., Kawata, D., Driver, S. P., & Gibson, B. 2007, Adv. Space Res., 9163, 001
Wolf, C., Wisotzki, L., Borch, A., Dye, S., Kleinheinrich, M., & Meisenheimer, K. 2003, A&A, 408, 499
Wyder, T. K., et al. 2005, ApJ, 619, L15
Yan, H., & Windhorst, R. A. 2004a, ApJ, 600, L1
———. 2004b, ApJ, 612, L93